PJEST

PJEST

Article

Design and Analysis of Multi-Layer Patched Efficient Antenna for 28-GHz Applications

Khalid Rehman[1,*], Iran Ullah[1], Yasir Ullah[1], Izaz Ahmad[1], Irfanud Din[2], Danish Shehzad[2]

[1] Electrical Engineering Department, CECOS University of Information Technology & Emerging Sciences, Peshawar, Pakistan; khalid@cecos.edu.pk
[2] Department of Computer Science, The Superior University, Lahore, Pakistan; danish.shehzad@superior.edu.pk
* Correspondence: khalid@cecos.edu.pk;

ABSTRACT: Microstrip antennas possess a compact form factor, exhibit a low profile, and demonstrate a lightweight nature, thereby enabling their suitability for deployment on both planar and non-planar surfaces. When the framework is installed, it requires a comparatively small amount of space. The production of printed circuits has become a facile and inexpensive process owing to advancements in contemporary technology. Antennas with a low profile are often required owing to space, weight, cost, performance, simplicity of installation, and aerodynamic profile in powerful planes, spaceships, satellites, and rocket operations. Many other applications, not only mobile radio and wireless communications, have comparable requirements. Microstrip antennas are a useful tool for accomplishing this goal. A proposal has been put forth to utilize a patch antenna for 5G cellular connectivity at 28 GHz, with the aim of generating robust beams on the azimuthal plane. The antenna proposed in this study exhibits a radiation efficiency of 93.46 percent and a total efficiency of 92.80 percent, as demonstrated through simulations. This study showcases the feasibility of producing millimeter-wave antennas operating at 28 GHz through the utilization of cost-effective additive manufacturing techniques. The simulation of all outcomes is conducted through the utilization of the CST Microwave Studio.

Keywords: Microstrip, 5G, 28 GHz, Radiation Efficiency, Millimeter-wave, CST Microwave.

Citation: Rehman, K., Ullah, I., Ullah, Y. ., Ahmad, I., Din, I., & Shehzad, D. Design and Analysis of Multi-Layer Patched Efficient Antenna for 28-GHz Applications. *Pakistan Journal of Emerging Science and Technologies (PJEST)*, 4(3). https://doi.org/10.58619/pjest.v4i3.123

Academic Editor: Dr. M. Javaid Afzal

Received date: 16th June, 2023
Revised date: 23th June, 2023
Accepted date: 24th June, 2023
Published date: 28th June, 2023

Pakistan Journal Emerging Sciences and Technologies (PJEST) in collaboration with Govt. Islamia College Civil Lines Lahore, Pakistan is licensed under a Creative Commons Attribution-ShareAlike 4.0 International License

Introduction:

The last few decades have witnessed significant advancements in mobile communications. It is expected that the implementation of 5G networks will occur in the initial stages of 2020–21. The advanced 5G network is characterized by high data rates, large bandwidth, minimal fading, and diverse communication capabilities among various devices. Studies have shown that the millimeter (mm) and centimeter (cm) wavebands may provide greater bandwidths than the third- and fourth-generation (3G and 4G) frequency bands. The WRC-15 conference was convened to deliberate upon the prospective expansion of IMT (International Mobile Telecommunications) infrastructure. The conference reached the resolution that mobile frequency bands ought to be situated within the range of 24.25 to 86 GHz [1]. The 28 GHz resonance frequency offers numerous supplementary advantages. In order to facilitate NLoS communications, it is practical and easy to provide varying route conditions during high-frequency operations. The 28 GHz frequency spectrum is also seen as a key enabler for the introduction of 5G services in real-world contexts. During the PyeongChang Winter Olympic Games in 2018, a trial was conducted on 5G consumer devices utilizing a 28 GHz frequency band [2]. Antennas for both mobile devices and base stations have been the subject of substantial research in the

context of 5G technology [3, 4]. Using lower 4G frequencies may help overcome the problem of considerable route loss in mm-wave bands, which is one of the key hurdles in antenna design. Due to the increased route loss and stoppage encountered at millimeter-wave frequencies, the signal-to-interference-plus-noise ratio (SINR) may be greatly improved by comparing systems at microwave frequencies. In cases where a line-of-sight (LOS) connection is present, point-to-point (P2P) broadcasting in the millimeter-wave frequency band is employed as a means of mitigating this loss. The selection process involves opting for a high-gain antenna and a highly directional beam, as referenced in sources [5] and [6]. Typically, a microstrip patch antenna consists of four constituent parts, namely the patch, ground plane, substrate, and feeding component. The estimation of input impedance for the radiation pattern can be achieved by determining the frequency. The term "patch" denotes a narrow metallic strip that exhibits non-conductive properties and is situated on a singular surface of a slender substrate. The metallic material present on the ground plane exhibits identical properties to the one situated on the opposing side of the substrate. The thickness of the substrate layer falls within the range of 0.01 to 0.05 times the wavelength of the electromagnetic wave in a vacuum. The principal purpose of this constituent is to furnish mechanical reinforcement and serve as an interstice amid the patch and its corresponding ground plane. When combined with materials possessing high dielectric constants, it is commonly employed to load the patch and reduce its dimensions.

DESIGN PROCEDURE:

The formula (1) for determining an effective radiator width that results in favorable radiation efficiencies is expressed as

$$w = \frac{1}{2f_r\sqrt{\varepsilon_0\mu_0}}\sqrt{\frac{2}{\varepsilon_r+1}} = \frac{v_0}{2f_r}\sqrt{\frac{2}{\varepsilon_r+1}} \qquad (1)$$

The symbol v_0 denotes the speed of light in a vacuum.

The formula (2) can be utilized to determine the effective dielectric constant of the microstrip antenna.

$$\varepsilon_{eff} = \frac{\varepsilon_r+1}{2} + \frac{\varepsilon_r-1}{2}\left[1+12\frac{h}{w}\right]^{-1/2} \qquad (2)$$

Upon obtaining the value of W through the aforementioned equation, the extension of length ΔL can be determined by utilizing the formula (3)

$$\frac{\Delta L}{h} = 0.412 \times \frac{(\varepsilon_{reff}+0.3)\left(\frac{w}{h}+0.264\right)}{\varepsilon_{reff}-0.258)\left(\frac{w}{h}+0.8\right)} \qquad (3)$$

The calculation of the patch length can be determined by solving the previously mentioned equation for the variable L, as it is represented by the following expression (4):

$$L = \frac{1}{2f_r\times\sqrt{\varepsilon_0\mu_0}\times\sqrt{\varepsilon_{reff}}} - 2\Delta L \qquad (4)$$

Simulation tools are software programs used to create virtual models of real-world systems. These tools allow users to test and analyze the behavior of a system under different conditions without the need for physical prototypes. Simulation tools are widely used in various fields, including engineering, science, and business, to optimize designs, improve performance, and reduce costs.

CST:

The mentioned computational tool exhibits proficiency and precision in resolving diverse antenna configurations. [1]

Objectives of the research:

The main aim of this research is to develop and assess a patch antenna operating at high frequencies that demonstrates exceptional radiation efficiency. The proposed high-band antenna operates at a frequency of 28 GHz, which is commonly considered the most suitable frequency for 5G technology.

Accomplishments:

To attain optimal implementation, we focused on achieving effectiveness in total efficiency, radiation efficiency, S-parameter, and antenna gain. This section provides an overview of the research conducted. The present study has been structured in a manner that enables graduate, BSc, and master's students to comprehend the research findings presented in this paper and derive benefits from them. The present study's organizational structure is as follows:

The problem statement is the central issue or concern that the research aims to address. The statement offers a succinct and unambiguous exposition of the subject matter that the research aims to explore. The current focus of research in 5G antenna design is centered on achieving high total efficiency and radiation efficiency in order to address issues such as low data rates, path losses, and heavy traffic for both personal and commercial applications.

POSSIBLE APPLICATION OF THE PROPOSED METHOD

The current investigation is centered on the design and implementation of a high-frequency patch antenna. A rectangular patch antenna was created specifically for 5G applications, with consideration given to the resonant frequencies of the technology. To accurately evaluate the properties of a material, it is essential to consider three critical factors: the resonant frequency, the relative permittivity of the material, and the thickness of the material. As per a cited source, the anticipated frequency ranges for 5G technology fall between 26.5 and 30 GHz. The primary objective of the current antenna model is to enhance efficiency for 5G applications, which is accomplished by modifying antenna characteristics based on a comprehensive review of recent research. Various techniques are available for constructing a high-frequency antenna [7].

The suggested approach for fabricating a patch antenna utilizing a solitary strip feedline entails the utilization of five radiating patches that are systematically arranged on a rectangular patch. The antenna proposed has been designed and simulated utilizing CST software. The current patch antenna is illustrated in Fig. 1. and Fig. 2. which display its frontal and three-dimensional viewpoints, respectively. The ground plane of the antenna under consideration is situated on the lowermost layer of the substrate. A Taconic TLY-5 substrate with a thickness of 0.79 mm has undergone etching to produce a rectangular patch. The positioning of the feedline is situated on the topmost stratum of the substrate. The Taconic TLY-5 substrate is utilized with a feeding layer thickness of h = 0.79 mm and an antenna sheet length of L1 = 4.32 mm, while r = 2.2. Table 1 displays the recommended dimensions for the antenna.

The proposed model's noteworthy design proposition can be succinctly summarized as follows:

The WR-28 rectangular waveguide is utilized to energize the feed line in a conventional manner. The Taconic TLY-5 substrate is utilized as the optimal substrate for high-frequency applications. The ground plane is constructed from aluminum, while the patches utilized for radiation conduction are composed of copper and lead, chosen for their high conductivity. The five radiating patches are relatively short, resulting in suboptimal gain during radiation transmission. Two parasitic patches have been incorporated, which are being supplied by the central patches. By implementing this method, it is possible to enhance both the bandwidth and gain of the antenna. The table presented below, denoted as Table (1) and contains all the relevant parameters.

The rest of the paper is divided into several sections. Section II focuses on Contributions to Research, highlighting the novel aspects of our work. In Section III, we study Related Work, where we review relevant literature to enhance our understanding and refine our research. Section IV is dedicated to Methodology, where we provide detailed examples of our approach. Moving on to Section V, we present the Simulation Results and Performance Evaluations, offering insights into the effectiveness of our methods. Section VI concludes with the Conclusion and Future Work, summarizing our findings and outlining potential areas for further exploration. Finally, the References section provides a comprehensive list of the sources cited throughout the paper.

Contributions to Research

The principal contribution of this study lies in its ability to devise a design that exhibits optimal performance in terms of total efficiency, radiation efficiency, S-parameters, and antenna gain. Over the course of recent decades, there has been a rapid advancement in mobile communication systems. The subsequent generations have consistently exhibited enhanced performance capabilities. Current 4G networks may provide peak data speeds in excess of 1 Gbps, paving the way for the introduction of a wide variety of useful and compelling new services including wireless video calling, remote home monitoring, and machine-to-machine interactions. The antenna system consists of five radiating patches, a waveguide, and a waveguide-to-microstrip line transition. The substrate utilized for the line and patches is a commercial Taconic TLY-5 with a thickness of 0.79mm. The input wave is introduced into the waveguide through the utilization of the fundamental mode

TE10. Subsequently, the signal is conveyed to the WMLT. A narrow rectangular probe was utilized and directly affixed to the substrate. The wave propagates through the 50-ohm transmission line and subsequently emits radiation via the five radiating patches. The arrangement of the five patches that emit radiation comprises a central patch that has been truncated, two patches that are parasitic in nature, and two side stubs that are open-ended. The antenna simulation employs the parameters outlined below:

The impedance of an electrical circuit refers to the resistance it offers to the current flow upon application of a voltage. It is necessary for the impedance of both the antenna and transmission cable to be identical, with a standard impedance value of 50. In cases where the impedance is not matched, a matching circuit is employed to align the impedance of the antenna and transmission cable. The parameter being discussed is the return loss, also known as S11. The ratio between the power reflected by the antenna and the power supplied to the antenna. The following equations demonstrate the return loss of the input port. The variable Vf represents the forward voltage that is propagated along the transmission line, while Vr denotes the reflected voltage.

$$S_{11} = \frac{v_f}{v_r} = \frac{z_L - z_0}{z_L + z_0} \qquad (5)$$

In equation (5), Z_L denotes the load impedance, whereas Z_0 represents the impedance of the broadcast line. The logarithmic quantity used to express S_{11} is known as the return loss of the input, denoted as in equation (6) RL_{input}.

$$RL_{input} = -20log_{10}|S_{11}|\ db \qquad (6)$$

Bandwidth is a technical term that pertains to the volume of information that can be conveyed through a communication channel or network within a specific timeframe. The term "bandwidth" in relation to an antenna denotes the spectrum of frequencies within which the antenna can function accurately. The antenna under consideration provides a bandwidth of 1.158 GHz when operating at a frequency of 28 GHz. The radiation pattern is a crucial aspect of antenna performance.

The radiation or antenna pattern exhibits the relative magnitude of the emitted field in different directions from the antenna while preserving a uniform distance. The antenna must possess the capability to cover the suggested frequency ranges while exhibiting minimal feed port impedance mismatch and sufficiently high radiation efficiency. The input impedance of an antenna in equation (7) is a significant parameter.

$$Z_{in} = R_{in} + jX_{in} \qquad (7)$$

$$R_{in} = R_R + R_L \qquad (8)$$

Equation (7) represents the input impedance that is perceived at the antenna's feed point. The component R_{in} in equation (8) can be bifurcated into two discrete resistive constituents, specifically the radiation resistance and the loss resistance. The absence of

the X_{in} component in the input impedance of the high-band antenna under consideration is attributed to resonance.

The concept of directivity is a crucial aspect of the field of acoustics. The directional capability of an antenna refers to its ability to focus a beam in a particular direction during transmission or to receive energy with greater precision from a specific direction during the reception. The power density can be calculated when the antennas are equidistant at a distance denoted by "r." Consequently, the component of directivity in equation (9) denoted as D is

$$D = \frac{F_{max}}{F_i} \qquad (9)$$

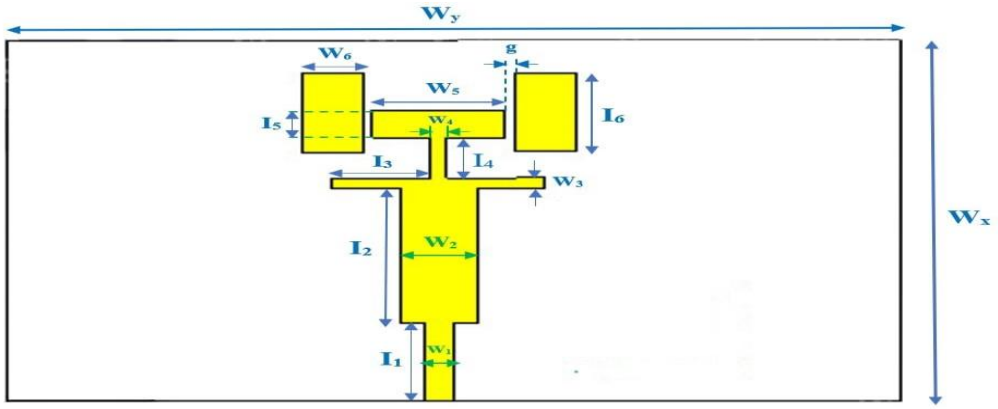


Fig. 1. The front view of the antenna design

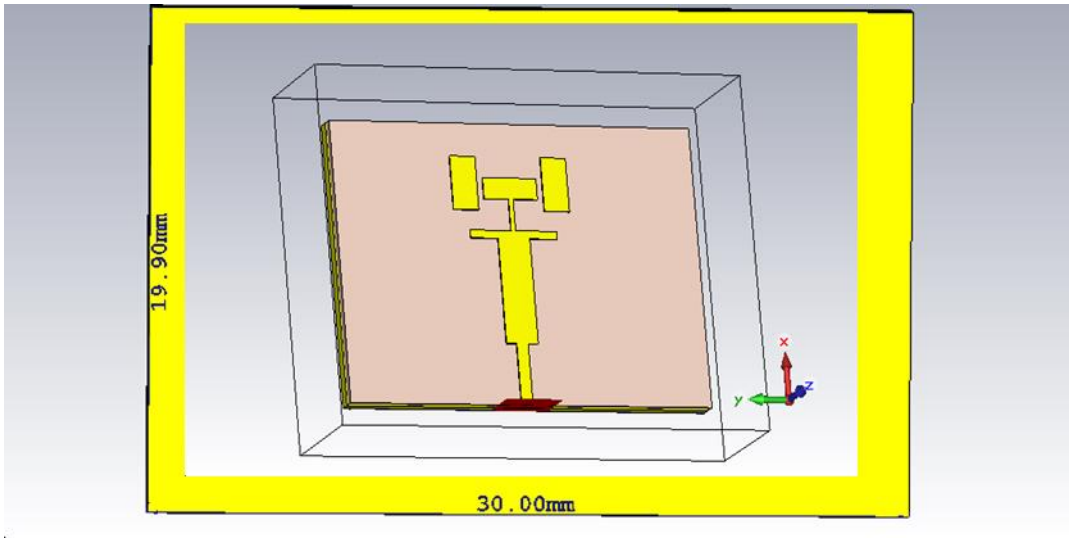


Fig. 2. Dimensional view of the antenna design

RELATED WORK

Comparison of various models

Table (2) provides a comparative evaluation of the antenna component in comparison to recently printed high-band antenna projects. The objective is to assess the performance of the proposed high-band antenna in relation to the current projects. The present designs exhibit instability in contrast to the anticipated radiation efficiencies and maximum gains. The design has yielded consistent antenna gains exceeding 5 dB and radiation efficiency surpassing 80% for the specific frequency bands under consideration. The primary cause can be attributed to the uniform field distributions that envelop the antenna. The antenna under consideration exhibited a simplistic configuration, rendering it advantageous for pragmatic implementations.

TABLE 1. Proposed antenna dimensions and parameters

Parameter	Dimension (mm)
W_x	19.9
W_y	30
l_1	4.32
l_2	7.43
l_3	3.3
l_4	2.23
l_5	1.5
l_6	4.35
W_1	0.95
W_2	2.64
W_3	0.56
W_4	0.57
W_5	4.45
W_6	2.1
H	0.79

L_p	2.2
ε_r	2.2
G	0.25

METHODOLOGY

Analysis and Presentation of Experimental Findings

The antenna under consideration has been devised and modeled utilizing the prescribed parameters. Upon performing a simulation, a variety of outcomes were acquired and analyzed, encompassing VSWR, return loss, directivity, gain, efficiencies, E-field, surface current distributions, and radiation performance. The following section provides a discussion of the aforementioned results.

TABLE 2. Comparison Of the Proposed Antenna with other Antennas

References	Radiation Efficiency (%)	Total Efficiency (%)	Gain in dB
Sub-mm wave array antenna[8]	79	90	12
Dielectric patch array antenna[9]	88.5	88.8	12.48
Dielectric patch array antenna[9]	78.2	76	11.61
Dual band printed slot antenna[10]	91.7	91	4.2
Compatible based array antenna[11]	95	80	13
3D-convege phased array antenna [12]	92	91.9	10
Steerable 28 GHz array antenna[13]	88	87	12.6
Umbrella shape patch antenna[14]	92.2	91	7.88
Compact dual band patch antenna[15]	62	61	7.71
Dual band FIPA antenna[16]	69	…	3.75
Slot directive antenna[17]	73	72	6.6
MM wave MIMO antenna[18]	77	76	6-8
Slot circular patch antenna[19]	85.6	…	7.6
Millimeter-wave antenna arrays[20]	80	79.53	26
Terahertz SIW slot antenna[21]	76.27	…	4.9
MIMO antenna array[22]	88.58	87	11.33
Compact slotted microstrip antenna[23]	82.08	…	8.735
Arc slot antenna[24]	82	81	17.2
Proposed result	93.46	92.80	6.566

The concept of return loss

Achieving high return loss across a broad frequency spectrum poses a significant challenge. In the scenario of a wideband, it is possible that the antenna-matching components could experience significant losses. The proposed antenna's high and wide

bands result in a notable improvement in return loss for 5G applications. The mathematical expressions below are utilized to represent the return loss of an input port, where Vf represents the voltage that is launched down the line in the forward direction and Vr represents the voltage that is reflected.

$$S_{11} = \frac{v_f}{v_r} = \frac{z_L - z_0}{z_L + z_0} \qquad (10)$$

Equation (10) denotes that Z_L represents the load impedance, while Z_0 represents the impedance of the broadcast line. The logarithmic quantity for S_{11}, which is the return loss RL_{input}, is expressed in equation (11) as RL_{input}.

$$RL_{input} = -20log_{10}|S_{11}|\ db \qquad (11)$$

The antenna proposed is depicted in Fig. 3. with clear resolution as a high-frequency antenna. At the resonant frequencies of 28 GHz, the return loss measures -36.87 dB. The 5G network operates within a frequency range spanning from 20 GHz to 1 THz. The frequency of 28 GHz is widely considered the most suitable for 5G technology, as it has the potential to effectively manage forthcoming cellular connectivity requirements.

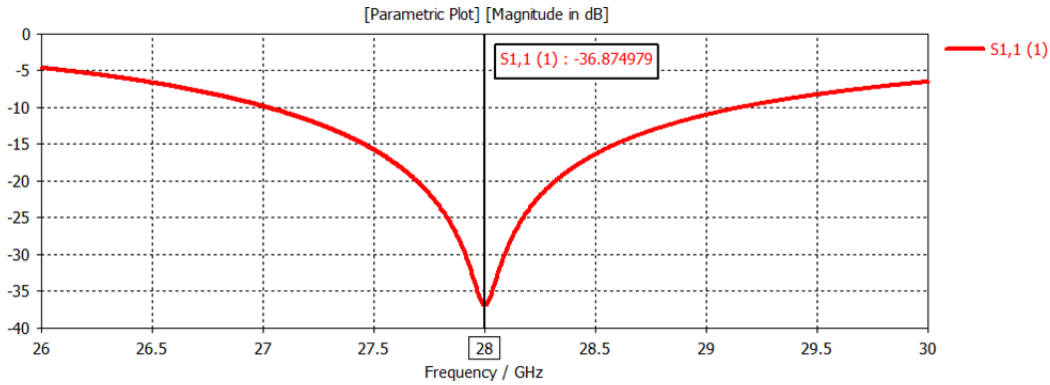


Fig. 3. The rear view of the antenna design

The concept of directivity

The estimation of power density is feasible under the condition that the antennas are positioned at an equal distance, which is represented by the variable "r." The directivity element, denoted by D, can be mathematically represented as the quotient of the maximum radiation intensity, Fmax, and the radiation intensity at a specific location, Fi. The value of Fi can be determined by dividing the transmitted power, Pt, by 4π, as demonstrated in equation (12).

$$D = \frac{F_{max}}{F_i} \quad \text{where} \quad F_i = \frac{P_t}{4\pi} \qquad (12)$$

The equation denoted as (8) specifies that Fmax represents power density, Pt denotes radiated power, and Fi signifies radiation intensity.

SIMULATION RESULTS AND PERFORMANCE EVALUATION

The utilization of parasitic patches is being employed to augment the effectiveness of the proposed patch. The findings of the simulations suggest that the implementation of this approach has resulted in an increase in antenna gain, directivity, and radiation efficiencies shown in Fig. 10. The equation (13) for determining the overall directivity capacity is expressed as follows:

$$D\ array\ (\theta, \phi) = AF \times D\ (\theta, \phi) \qquad (13)$$

where D (θ, ϕ) represents the directivity of an individual component. The monosyllabic term in question is occasionally denoted as the design element. Fig. 4. illustrates the prevailing antenna directivity at a frequency of 28 GHz. Based on the three-dimensional analysis of the antenna, it has been determined that the path of radiation is situated along the positive y-axis. At the specified frequency, the antenna exhibits a directivity of 6.9 dBi.

GAIN OF ANTENNA:

As per Balanus, the amplification can be mathematically represented as the multiplication of directivity and efficiency. The mathematical expression for the gain of an antenna can be represented as the outcome of multiplying the directivity of the antenna by its efficiency.

Antenna Gain = Directivity × Antenna Efficiency

The expression denoted as Equation (14) represents the complete power emitted by an antenna in the form of a surface integral. The distance d is the R.M.S. field power in free space, which is represented by E. The integral is defined in a precise manner.

$$F_i = \frac{d^2}{120\pi} \int_0^{2\pi} \int_0^{\pi} \qquad (14)$$

Equation (15) specifies the gain relative to an isotropic antenna when En represents the field strength in a specific direction. The gain, denoted as gi, is calculated as follows:

$$g_i = \frac{4\pi E_n^2}{\int_0^{2\pi} \int_0^{\pi} E^2 sin\theta d\theta d\varphi} \qquad (15)$$

The variable labeled as "Gi" signifies the amplification that is exclusively ascribable to the directional attributes of an antenna's radiation pattern. The antenna under consideration incorporates effective design principles to minimize electrical losses to a practical degree. The necessity of beam formation arises from the high density of the 5G network and the path loss in the millimeter wave spectrum. High-gain millimeter-wave beams can effectively mitigate the impact of greater path losses, thereby resulting in reduced power

demands for individual users. According to the data depicted in Fig. 4., the projected antenna gains for the 28 GHz frequency amount to 6.566 dBi. The antenna gain criterion is considered to be superior in relation to the performance of the proposed antenna, which demonstrates directional radiation characteristics. Furthermore, it has been observed that the gain at a frequency of 900 is achieved at a level of 6.565 dBi on the 28 GHz spectrum. Despite the presence of tolerances leading to certain disparities between the imitated and computed outcomes, the simulation and observational procedures predominantly yielded a high degree of concurrence. The antenna proposed in the study demonstrated favorable matching characteristics, with S11 values below -10 dB across all frequencies of operation, as illustrated in the accompanying figure. The gain patterns that were measured are presented in Fig. 5. specifically at a frequency of 28 GHz. It is evident that the radiation efficiency is favorable within the frequency range of maximum amplitude. The E-plane, situated at an azimuth angle of zero degrees, demonstrates a far-field arrangement that manifests an asymmetrical characteristic. The antenna's gain was increased through a technique of reducing the signal's concentration along the vertical axis while emphasizing its concentration along the horizontal axis.

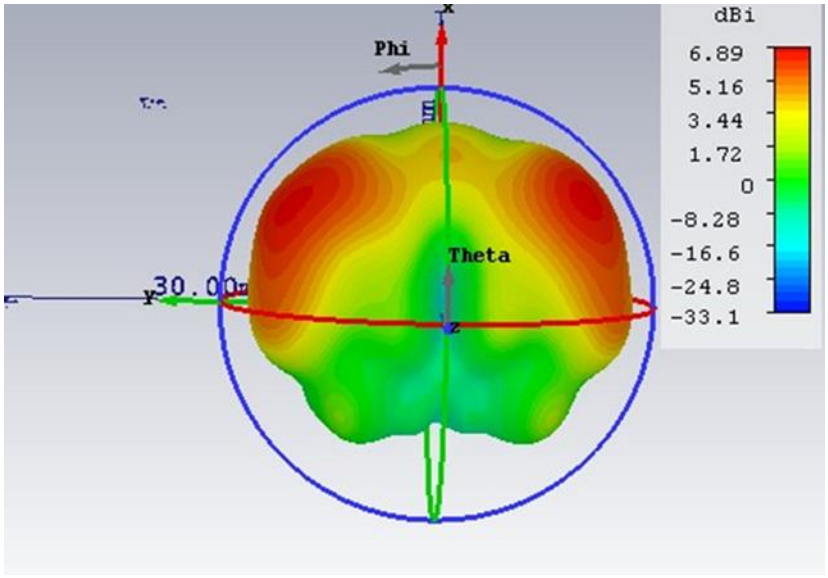


Fig. 4. Directivity and Gain of proposed antenna at 28 GHz

RADIATION PERFORMANCE

Fig. 4. depicts the energy pattern of the antenna with respect to directivity, while the radiation pattern for gain is illustrated in the aforementioned figure. The antenna is required to have the ability to cover all the desired frequency ranges while simultaneously maintaining a low feed port impedance matching and demonstrating a sufficiently high radiation performance. The parameter of utmost significance in an antenna is its input impedance.

$$Z_{in} = R_{in} + Jx_{in} \quad (16)$$

$$R_{in} = R_R + R_L \quad (17)$$

Equation (16) expresses the impedance Zin as the sum of the real part Rin and the imaginary part jXin. Equation (17) defines the real part R_{in} as the sum of the resistance RR and the inductive reactance(RL). Equation (16) denotes the impedance that is observed at the antenna's feed point. The actual component of Rin can be partitioned into two distinct parts, namely the RR radiation resistance and the RL loss resistance. The resonance operation of the proposed high-band antenna results in the absence of the Xin component in its input impedance. As illustrated in Fig. 8. the real component of impedance converges to 86, indicating a transfer of maximum power to the radiated patch antenna. Likewise, with regards to the imaginary component of impedance, the depicted Fig. 7. illustrates a value in close proximity to zero. A resonance state is declared for an antenna that possesses a zero imaginary component. Hence, it is imperative that the impedance requirement for the antenna be neither excessively high nor excessively low in order to ensure accurate operation. In contrast to the patch antennas utilized in prior research, the antenna under consideration exhibits superior vertical cross-separation characteristics and a consistent energy radiation pattern. The utilization of metamaterials in antenna design results in larger dimensions to address this concern and minimize the dimensions of the antenna, a substrate featuring an elevated dielectric constant has been utilized. According to the modeling outcomes, the directivity's energy form exhibits a principal lobe situated at an angle of 56 degrees when the frequency is 28 GHz. Likewise, at this specific frequency, the primary lobe's magnitude is 5.42 decibels in relation to an isotropic radiator (dBi)., with the adjacent sections exhibiting a degree of -3.3 decibels (dB). The energy distribution of an antenna's gain exhibits equivalence to directivity, except for the magnitude of the main lobe at 28 GHz, which registers a gain of 5.1 dB at an angle of 56 degrees. Additionally, the far-field arrangements display certain irregular peculiarities, specifically in the electric field plane at an azimuthal angle of 0 degrees.

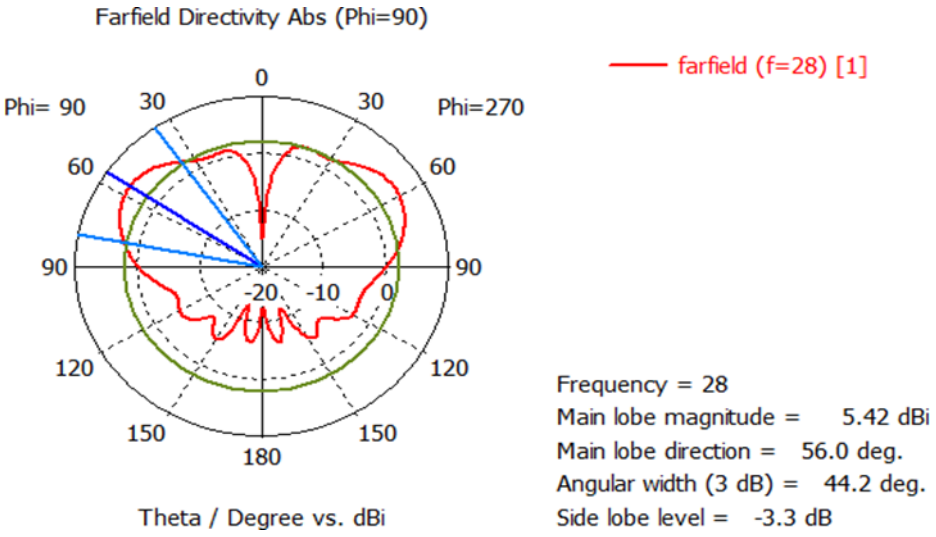


Fig. 5. Radiation Pattern for Directivity and Energy Pattern for Gain of proposed antenna at 28 GHz

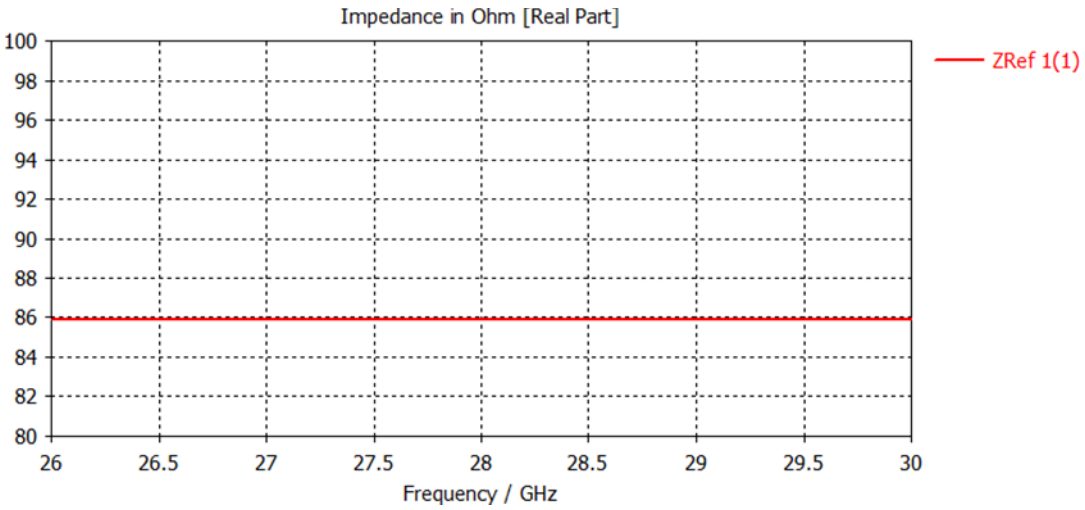


Fig. 6. The real part of the reference impedance of the proposed antenna

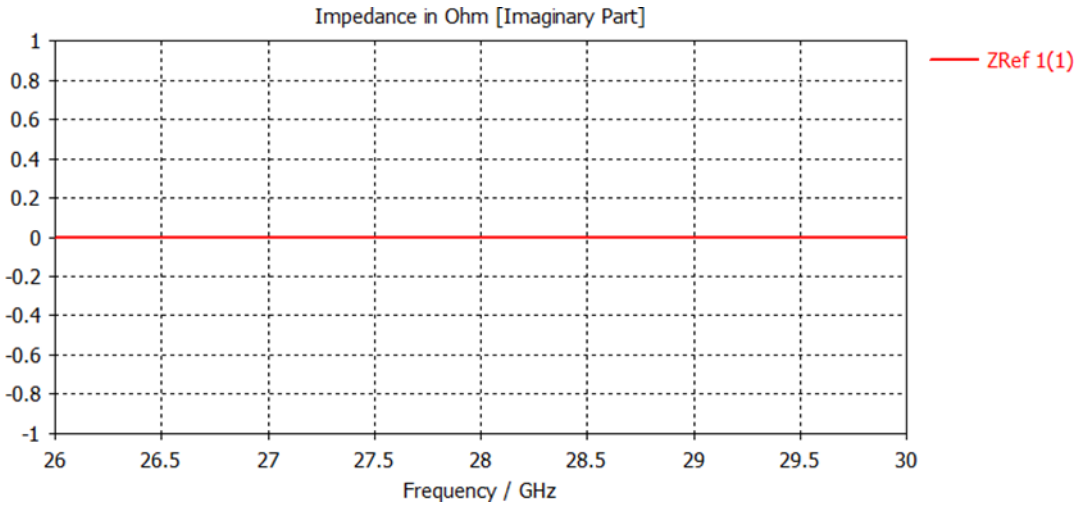


Fig. 7. The imaginary part of the reference impedance of the proposed antenna

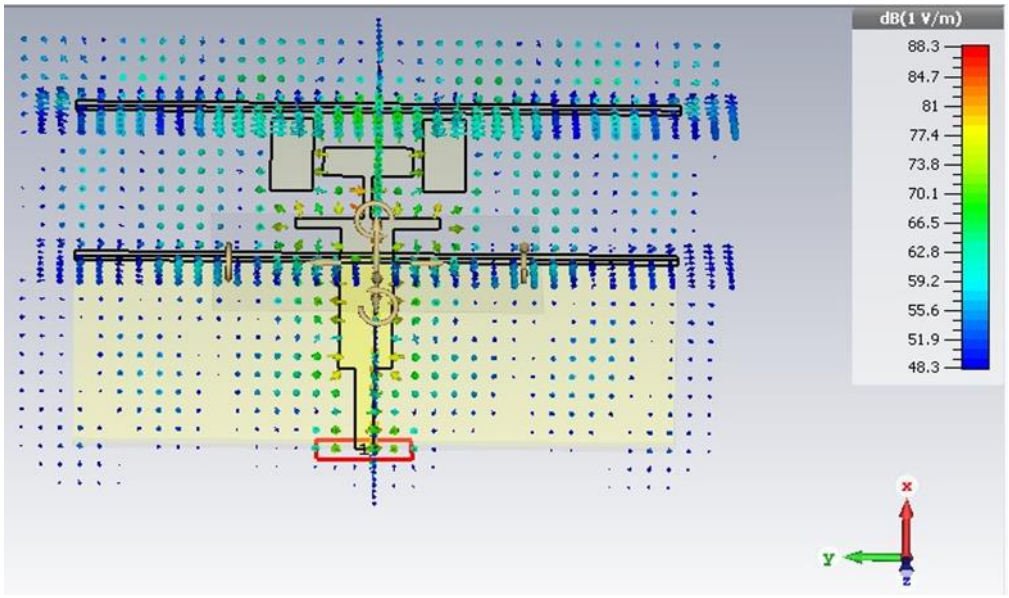


Fig. 8. E-Field Distribution in the proposed antenna at 28 GHz

E-FIELD

The Fraunhofer distance, denoted by d_f and expressed in equation (18) as:

$$d_f = \frac{2D^2}{\lambda}\ , \qquad (18)$$

is a metric employed to characterize the near- and far-fields. The variable D represents the diameter of the antenna. At the center of the patch, the electric field exhibits a null value, while on one side it attains its maximum value and on the other side it reaches its minimum value, with the lowest value being observed in the intermediate region. The occurrence of electric-pitch scattering at a frequency of 28 GHz is depicted in Fig. 8. The patch encounters a substantial electric field at a frequency of 28 GHz, affecting both its upper and lower surfaces.

Scattering of surface currents

The antenna under consideration presents a viable option that is both economical and spatially efficient for facilitating high-band communication, operating within a frequency spectrum of 28 GHz.. The antenna patch exhibits elevated scale at its extremities and notable current sharing that initiates at the patch's midpoint during resonance frequency. Changes in the height of the substrate result in significant alterations in the scattering phenomenon. Fig. 9. displays the surface current scatterings that were measured at resonance frequencies of 28 GHz. In order to attain the desired radiation pattern, it is necessary to modify the surface current through the incorporation of slots. As anticipated, the stream flowed vigorously beyond the confines of the patch. The augmentation of the electrical dimensions of the intended antenna through the implementation of an aperture results in the redirection of current flow towards the enhanced geometry that has been established.

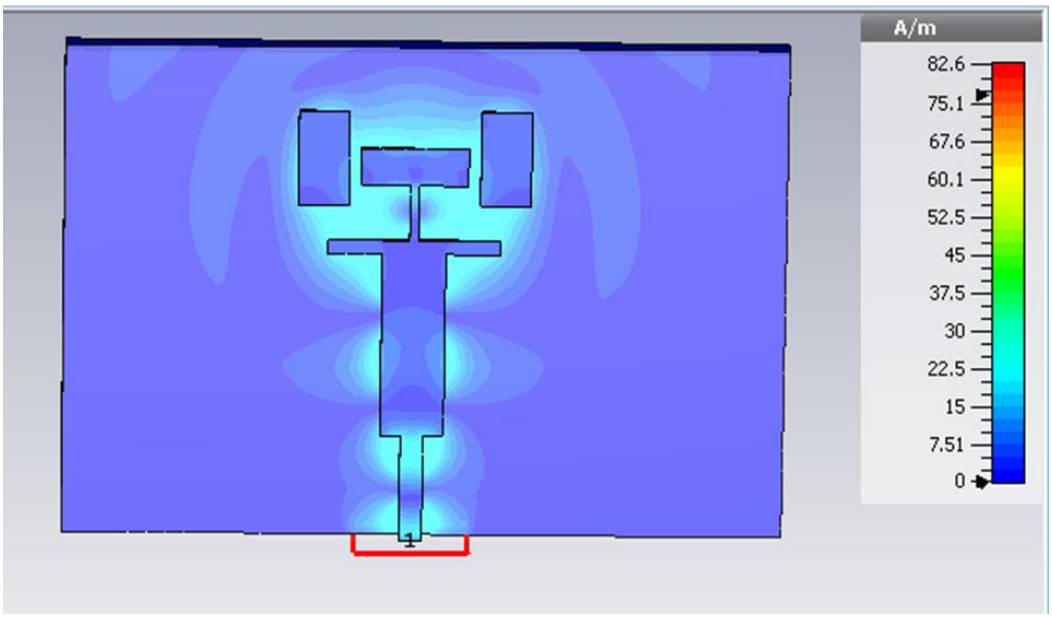


Fig. 9. Surface Current Scattering of the antenna at the resonating frequency

ANTENNA EFFICIENY

The antenna's efficiency can be mathematically represented as the multiplication of its matching loss and radiation efficiency, denoted as εT and given by the equation εT = ML · εR, where ML and εR represent the matching loss and radiation efficiency, respectively.

The variable ML is utilized to represent the loss that is sustained by the antenna due to impedance mismatch. On the other hand, the symbol η is utilized to denote the efficiency of the antenna. An antenna with high radiation efficiency can efficiently transmit input power to the surrounding free space. In instances where the radiation efficiency is diminished, a considerable fraction of the input power is expended as a

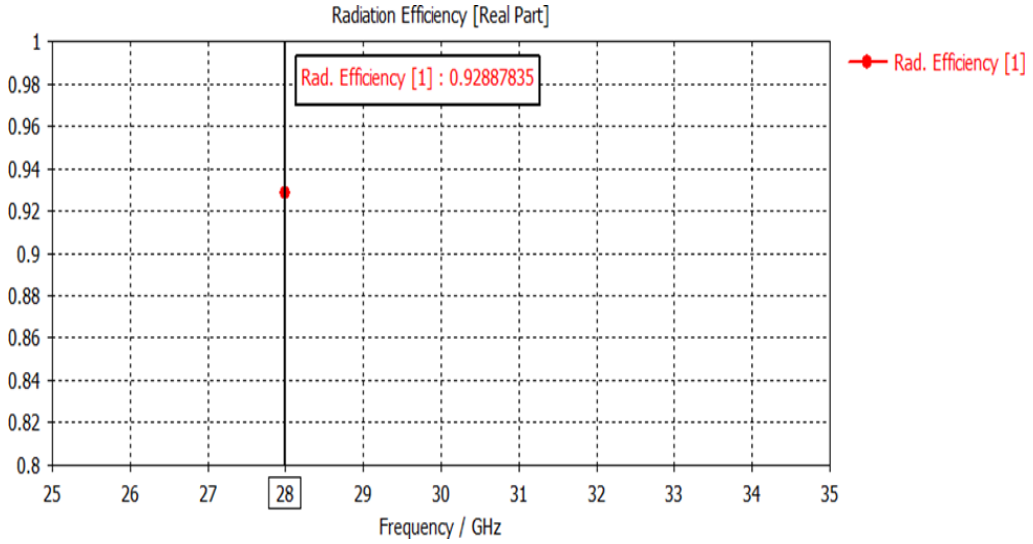


Fig. 10. Radiation Efficiencies of the antenna

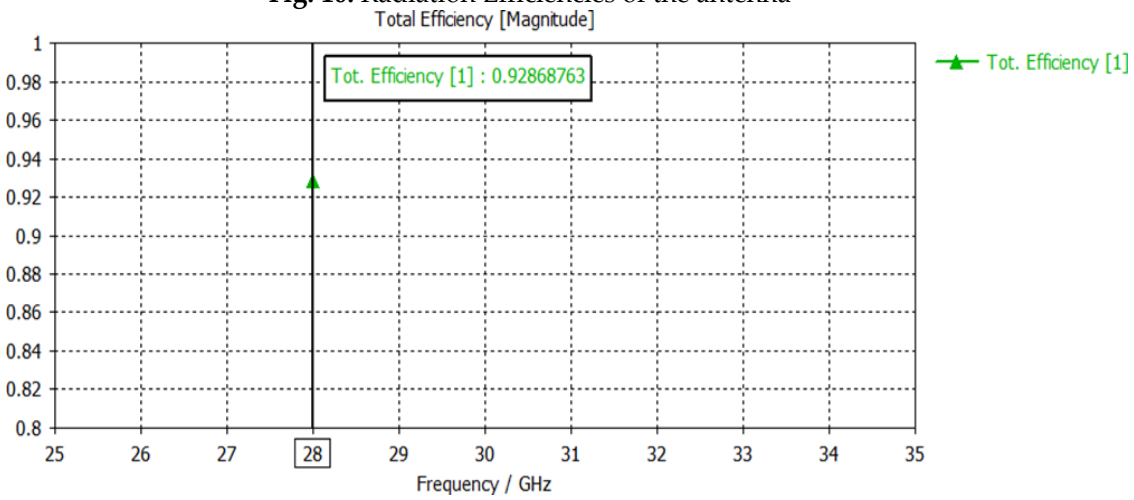


Fig. 11. Total Efficiencies of the antenna

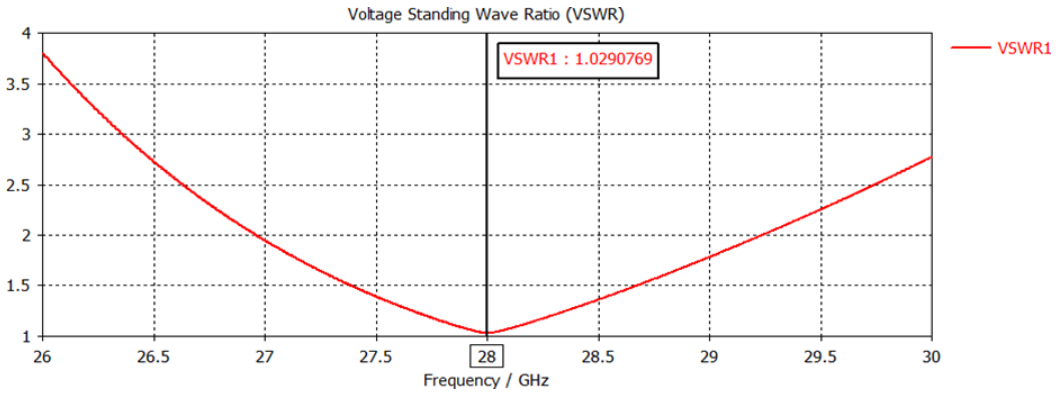


Fig. 12. VSWR of the Antenna

result of internal losses, including metal conduction, dielectric losses, and magnetic losses that occur within the antenna. Quantifying the transmission and dielectric losses of an antenna is a challenging task in the field of antenna engineering, albeit sporadically assessed through measurement. Despite being challenging to differentiate during measurement, they are often amalgamated to constitute the conduction dielectric efficacy. In general, the efficacy of Wi-Fi or mobile phone antennas is considered to be exceptional. The principal aim of our investigation was to determine the radiation efficiency and overall efficiency of the suggested antenna. Our findings indicate that the radiation efficiency and total efficiency shown in Fig. 11. were 92.89 and 92.85, respectively.

The assessment of the voltage standing wave ratio (VSWR) of the antenna in question is currently underway. Fig. 12. depicts the fluctuation of the voltage standing wave ratio (VSWR) specifically at resonant frequencies of 28 GHz. It can be observed that the VSWR values are below two for all frequencies and tend towards unity.

CONCLUSION AND FUTURE WORK

CONCLUSION

In conclusion, this study has provided valuable insights into the topic at hand. However, there is still much room for further research in this area. Future work could focus on exploring additional variables that may impact the results as well as conducting longitudinal studies to track changes over time. Furthermore, it would be advantageous to examine the extent to which these results can be applied to diverse populations and settings. In general, this study provides a basis for subsequent investigations in this particular area of study. To summarize, based on the aforementioned factors, it can be concluded that the high-band antenna has undergone demonstration, optimization, and simulation through the utilization of CST Microwave Studio. The antenna under consideration exhibits a less complex configuration in comparison to the presently employed wideband antennas. Comparable enhancements have been implemented for the suggested antenna's impedance bandwidth, intricacy, and expenditure. Furthermore, an increased level of radiation effectiveness is achieved. The implementation of high-frequency bands in broadband presentations has enabled the provision of auxiliary services with elevated data rates. The anticipated outcome suggests that the proposed antenna configuration demonstrates exceptional results in return loss, efficiency, antenna gain, and beam-forming capabilities across all operational frequency bands, rendering it appropriate for meeting the communication demands of fifth-generation (5G) millimeter wave technology. To summarize, the proposed high-frequency antenna exhibits enhanced efficacy owing to its adaptable antenna configuration. Additionally, it exhibits a significant level of amplification.

a. RESEARCH SUMMARY

Table II provides a concise overview of the calculations carried out to ascertain the resonant frequency, impedance bandwidth, return loss, and potential applications of the antenna being analyzed. This enables a clear understanding of the operational features of the antenna. The antenna's radiation pattern stability has been improved, resulting in a gain of 6.566 dB over the designated frequency range. A radiation effectiveness estimate

of at least 92.89% is achieved within the specified frequency range. The proposed high-band antenna exhibits superior and more uniform far-field radiation characteristics.

RESEARCH UTILIZATION

The utilization of research findings is a crucial aspect of academic inquiry. The utilization of the microstrip patch antenna configuration is recommended for cellular antenna design structures that prioritize a compact design and require a superior high-band solution. This design exhibits superior gain and efficiency while also providing optimal value for other antenna parameters when operating at high-band 5G frequencies.

FUTURE RECOMMENDATION

The utilization of efficient and expeditious simulation software such as CST MWS® has resulted in a reduction of workload for engineers and an acceleration of the antenna design process. Multi-band antennas that are small, low-profile, and highly efficient are widely utilized in various applications, including commercial, civil, military, and space-borne contexts. The development and enhancement of high-band antennas is a crucial field of study in the realm of antenna design and performance optimization. The practicality of antennas in cellular and weight-restricted constructions necessitates a small and conformal design. Further development can enhance the efficacy of microstrip antennas, including those utilized in the PCS. This study involves the analysis of the high-band antenna model through simulation. The alterations made to the width and length of the antenna substrate were conducted to investigate the impact on different antenna characteristics. A forthcoming research will showcase the methodology for incorporating the minute frequency deviations that arise from alterations to the antenna's dimensions, such as its width, length, or other attributes. Moreover, the consequences of the patch will be assessed across various frequency ranges concerning 4G LTE and mobile communication. To optimize the functionality of the antenna for cellular and weight-limited structures, it is imperative to implement a compact and conformal design. The efficacy of microstrip antennas, particularly those employed in PCS, can be improved through additional advancements in their development. The present investigation entails the examination of the high-frequency antenna prototype via computational modeling. The dimensions of the antenna substrate have been altered in order to examine the effects on various antenna properties. A forthcoming presentation will illustrate the process of incorporating the minor frequency deviations that arise from alterations made to the antenna's physical attributes, such as its width, length, or other properties. Moreover, an assessment will be conducted on the impact of the patch on diverse frequency ranges employed in 4G LTE and cellular telecommunications.

Author's Contribution: K.R. Conceived the idea; I.U., Y.U., & I.Z., Designed the simulated work and did the acquisition of data; K.R., I.U., Y.U., & I.Z., Executed simulated work, data analysis or analysis and interpretation of data and wrote the basic draft; I.D., & D.S., Did the language and grammatical edits & Critical revision.

Funding: The publication of this article was funded by no one.

Conflicts of Interest: The authors declare no conflict of interest.

Acknowledgment: We extend our heartfelt gratitude to the dedicated team for their invaluable collaboration in the data collection process. Their tireless efforts and unwavering commitment have been instrumental in the successful completion of this research paper.

REFERENCES

[1] CST Microwave Studio: Workflow Solver Overview. CST Studio 2015, CST-GmbH, 2015.

[2] Ko, Junghoon, Sooyoung Hur, Sunguk Lee, Youngseok Kim, Yun-Seok Noh, Yeon-Jea Cho, Shinhwan Kim et al. "28 GHz channel measurements and modeling in a ski resort town in Pyeongchang for 5G cellular network systems." In 2016 10th European Conference on Antennas and Propagation (EuCAP), pp. 1-5. IEEE, 2016.

[3] Hong, Wonbin, Kwang-Hyun Baek, Youngju Lee, Yoongeon Kim, and Seung-Tae Ko. "Study and prototyping of practically large-scale mmWave antenna systems for 5G cellular devices." IEEE Communications Magazine 52, no. 9 (2014): 63-69.

[4] Boccardi, Federico, Robert W. Heath, Angel Lozano, Thomas L. Marzetta, and Petar Popovski. "Five disruptive technology directions for 5G." IEEE communications magazine 52, no. 2 (2014): 74-80

[5] Ando, Makoto, Jiro Hirokawa, Tetsuya Yamamoto, Akira Akiyama, Yuichi Kimura, and Naohisa Goto. "Novel single-layer waveguides for high-efficiency millimeter-wave arrays." IEEE Transactions on microwave theory and Techniques 46, no. 6 (1998): 792-799.

[6] Pi, Zhouyue, and Farooq Khan. "An introduction to millimeter-wave mobile broadband systems." IEEE communications magazine 49, no. 6 (2011): 101-107.

[7] Park, Jang-Soon, Jun-Bong Ko, Heon-Kook Kwon, Byung-Su Kang, Bonghyuk Park, and Dongho Kim. "A tilted combined beam antenna for 5G communications using a 28-GHz band." IEEE Antennas and Wireless Propagation Letters 15 (2016): 1685-1688.

[8] Mao, Chun-Xu, Mohsen Khalily, Pei Xiao, Tim WC Brown, and Steven Gao. "Planar sub-millimeter-wave array antenna with enhanced gain and reduced sidelobes for 5G broadcast applications." IEEE Transactions on Antennas and Propagation 67, no. 1 (2018): 160-168 (2018).

[9] Haraz, Osama M., Ayman Elboushi, Saleh A. Alshebeili, and Abdel-Razik Sebak. "Dense dielectric patch array antenna with improved radiation characteristics using EBG ground structure and dielectric superstrate for future 5G cellular networks." IEEE Access 2 (2014): 909-913.

[10] Haraz, Osama M., Mohamed Mamdouh M. Ali, Saleh Alshebeili, and Abdel-Razik Sebak. "Design of a 28/38 GHz dual-band printed slot antenna for the future 5G mobile communication Networks." In 2015 IEEE International Symposium on

Antennas and Propagation USNC/URSI National Radio Science Meeting, pp. 1532-1533. IEEE, 2015.

[11] Ojaroudiparchin, Naser, Ming Shen, and Gert Frolund Pedersen. "A 28 GHz FR-4 compatible phased array antenna for 5G mobile phone applications." In 2015 International Symposium on Antennas and Propagation (ISAP), pp. 1-4. IEEE, 2015.

[12] Ojaroudiparchin, Naser, et al. "A switchable 3-D-coverage-phased array antenna package for 5G mobile terminals." IEEE Antennas and Wireless Propagation Letters 15 (2016): 1747-1750.

[13] Razali Ngah, T. A. Rahman, and Hamza M. R. AlKhafaji,"A Steerable 28 GHz Array Antenna Using Branch Line Coupler" Stella Ifeoma Orakwue *, (2018), INSPEC Accession Number: 15519934

[14] Iftikhar Ahmad; Sun Houjun; Qasim Ali; Abdul Samad,"Design of Umbrella shape single element patch antenna with high gain and high efficiency for 5G wireless communication in 28 GHz "2020 17th International Bhurban Conference on Applied Sciences and Technology (IBCAST) Year: 2020 | Conference Paper | Publisher:IEEE

[15] Jandi, Y., F. Gharnati, and A. O. Said, "Design of a compact dual bands patch antenna for 5G applications", 2017 International Conference on Wireless Technologies, Embedded and Intelligent Systems (WITS), 14, IEEE, April 2017.

[16] Ahmad, W. and W. T. Khan, "Small form factor dual-band (28/38 GHz) PIFA antenna for 5G applications", 2017 IEEE MTT-S International Conference on Microwaves for Intelligent Mobility (ICMIM), 21 24, IEEE, March 2017.

[17] Ali, M. M. M., and A. R. Sebak, "Dual-band (28/38 GHz) CPW slot directive antenna for future 5G cellular applications", 2016 IEEE International Symposium on Antennas and Propagation (APSURSI), 399,400, IEEE, June 2016.

[18] Thomas, T., K. Veeraswamy, and G. Charishma, " MM wave MIMO antenna system for UE of 5G mobile communication: Design", 2015 Annual IEEE India Conference (INDICON), 15, IEEE, December 2015. Sam, C. M. and M. Mokayef, A wide band slotted microstrip patch antenna for future 5G, EPH— International Journal of Science And Engineering (ISSN: 2454-2016), Vol. 2, No. 7, 19,23,2016.

[19] Muhammad Khattak, Ubaid Khan, Zakaullah and Gunawan witjaksono, "Elliptical Slot circlcular Patch Antenna Array with Dual Band behaviour for

future 5gmobile communication", Progress in Electromagnetic ResearchC-January,2019.

[20] Wu, Kai-lai, Yuan Yao, Xiao-he Cheng, Jun-sheng Yu, Tao Yu, and Xiaodong Chen. "Analysis and design of novel wideband and high-efficiency millimeter-wave antenna arrays for 60-GHz applications." Frontiers of Information Technology Electronic Engineering 21, no. 1 (2020): 128- 143.

[21] Sun, Peng-lin. "420-GHz terahertz SIW slot antenna with quartz superstrates in silicon technology." Optoelectronics Letters 16, no. 1 (2020): 25-28.

[22] Malviya, Leeladhar, Ajay Parmar, Deepak Solanki, Parul Gupta, and Priyanshi Malviya. "Highly isolated inset-feed 28 GHz MIMO-antenna array for 5G wireless application." Procedia Computer Science 171 (2020): 1286-1292.

[23] Merlin Teresa, P., and G. Umamaheswari. "Compact Slotted Microstrip Antenna for 5G Applications Operating at 28 GHz." IETE Journal of Research (2020): 1-8.

[24] Kim, Hyunjin, and Sangwook Nam. "28 GHz metal cavity-backed twin arc slot antenna for high efficiency and thermal management." Microwave and Optical Technology Letters